ELSEVIER

Polymer 42 (2001) 8769–8777

polymer

www.elsevier.com/locate/polymer

Synthesis and thermal characterization of crystallizable poly(caprolactone)/poly(hexamethylene terephthalate) block copolymer

C. Lefèvre[a], D. Villers[b], M.H.J. Koch[c], C. David[a,*]

[a]*Université Libre de Bruxelles, Chimie des Polymères et des Systèmes Organisés, Campus Plaine 206/1, Boulevard du Triomphe, B-1050 Brussels, Belgium*
[b]*Laboratoire de Physico-Chimie des Polymères, Université de Mons-Hainaut, 20, Place du Parc, B-7000 Mons, Belgium*
[c]*European Molecular Biology Laboratory, Hamburg Outstation, EMBL c/o DESY, Notkestrasse 85, D-22603 Hamburg, Germany*

Received 29 March 2001; received in revised form 18 May 2001; accepted 23 May 2001

Abstract

An alternating multiblock copolymer of poly(ε-caprolactone) (PCL) and poly(hexamethylene terephthalate) (PHT) with a 48/52 PCL/PHT composition weight ratio has been synthesized. Its structural and morphological parameters were measured using ^{1}H NMR, density measurements, differential scanning calorimetry and its crystallization and melting were studied by real time simultaneous WAXS and SAXS using synchrotron radiation. These results are compared with those for the pure PCL and PHT used as building blocks. In the crystallization conditions used here, the copolymer crystallizes as alternate lamellae of PHT and PCL. The crystallinity of the PCL blocks is much lower than that of pure PCL because they crystallize under stress in the semi-crystalline PHT network.

Keywords: Block copolymer; Poly(caprolactone); Poly(hexamethylene terephthalate)

1. Introduction

The primary purpose of this work was to synthesize a biodegradable polymer with good mechanical and thermal properties for use in packaging.

Poly(ethylene terephthalate) (PET) is widely used for these applications although its biodegradability is far from evident as proven by the variable degrees of degradation reported in the literature [1–4]. The data indicate that transformation of PET into fertilizer in industrial composting sites appearing throughout Europe is a hopeless undertaking. Environmental microbiology studies [5–9] have, however, demonstrated that model compounds such as esters of terephthalic, orthophthalic and isophthalic acids are assimilated by various microorganisms in the field as well as in the condition used in our laboratory [10]. This suggests that the poor biodegradability of PET resides in the physical properties of the material (rigidity of the chains and crystallinity) more than in the chemical structure of the building blocks. In contrast, like most aliphatic polyesters, poly(ε-caprolactone) (PCL) is quantitatively assimilated by a large variety of microorganisms [11,12] but has poor thermal and mechanical properties. Its blends with starch have been widely studied [13] and find increasing use in the production of composting bags for household refuse to be degraded in industrial composting sites. The preceding considerations suggest that statistical copolymers of aliphatic and aromatic units should have improved properties. This path has recently been investigated [14] and shown to be promising. The purpose of the present work is to study the behavior of alternating multiblock copolymers that could be rather easily synthesized on an industrial scale using di-isocyanate as junction units between blocks. Di-OH terminated PCL and poly(hexamethylene terephthalate) (PHT) have been chosen as building blocks. The choice of PHT is justified by the lower rigidity of the chains compared to PET. Its thermal properties and crystalline morphology have recently been comprehensively investigated [25]. In addition to its biodegradability, an exploratory study of the physical properties of an alternating multiblock copolymer presents an obvious interest as shown by the short survey of the state of knowledge on block materials below. The application of small-angle X-ray scattering (SAXS) and wide-angle X-ray scattering (WAXS) to amorphous and crystalline block copolymers has been reviewed recently [15]. Studies on amorphous, usually monodisperse, diblocks [16–18] have shown that below an order–disorder transition temperature (ODT), microphase separation into ordered structures occurs in the melt. This separation results from the segregation of

* Corresponding author. Tel.: +32-2-672-3009; fax: +32-2-650-5410.
E-mail address: christiane.david@village.uunet.be (C. David).

0032-3861/01/$ - see front matter
PII: S0032-3861(01)00362-7

incompatible components that are chemically linked. If one of the blocks is crystallizable [19–23], microphase separation can be due either to repulsive forces between segments in the homogeneous melt or to crystallization of the crystallizable component. The mechanism of phase separation and the final morphology depends on the relative values of the ODT and of the melting temperature. If the first one is higher than the second, crystallization occurs in the microphase separated melt while in the second case crystallization is the driving force for phase separation in the disordered melt. Triblock copolymers with two crystallizable components (PCL–PEG–PCL) and different lengths of the PCL blocks have been studied by Nojima et al. [24] and compared with blends of different compositions. Combining differential scanning calorimetry (DSC) and SAXS results, they showed that, in the blend, PEG and PCL segregate by crystallization, leading to individual domains where each component has its own lamellar structure. In the copolymer, large-scale segregation is not possible due to the chemical bonds between blocks. Nojima et al. proposed that when the weight fractions of the two components are comparable, they both crystallize forming an alternate lamellar structure of PEG and PCL. Alternating multiblock copolymers of two crystallizable components like the ones described below have to our knowledge never been studied.

2. Experimental

2.1. Copolymer synthesis

The copolymer was synthesized in two steps using di-OH terminated PHT prepared as previously described [25] and di-OH terminated polycaprolactone (PCL) 3000 kindly supplied by Solvay Interox. Toluene diisocyanate (TDI) was used as the junction unit. The first step involves the synthesis of a TDI terminated PCL prepolymer. The molecular ratio of TDI to PCL was chosen to be 2/1. The reaction was performed in bulk at 90°C. At this temperature, TDI and the catalyst (stannous octoate 0.1 wt% dry) are added to PCL. The reaction was stopped when the conversion, determined by measuring the number of free NCO in the reaction medium, reached 50% and the resulting prepolymer was diluted with the same volume of toluene. In this step, a solution of PHT 3400 was dissolved in *N*-methylpyrrolidone (30 wt%), heated to 90° in the reactor with 0.1 wt% dry stannous octoate. The dilute prepolymer was then added progressively to the reactor. When conversion attained 90% as measured by titration, the reaction medium was diluted and maintained at 90°C overnight. The fraction of residual NCO was then of the order of 5% of the initial OH and the reaction was stopped by addition of isopropanol. For titration of NCO groups, an excess dibutylamine (1N in dry dimethylformamide) was added to the polyester dissolved in toluene. After 10 min, unreacted dibutylamine was titrated with a methanolic 0.1N solution of HCl.

2.2. Molecular weight (MW) determination

The MW was determined by end group titration as previously described [25] or by GPC using a L-7350 Hitachi-Merck apparatus at 40°C with chloroform as solvent. Two mixed-D 5 μm PLgel (300 × 7.5 mm) linear between 200 and 40,000, calibrated with polystyrene standards were used at an elution rate of 1 ml/min.

2.3. DSC

DSC measurements were performed on a power compensating Perkin Elmer DSC-7 apparatus. To avoid oxidative degradation, the sample and reference pans were purged with nitrogen at constant flow rate. The temperature and melting enthalpy were calibrated using indium (T_m = 156.6°C; ΔH_m = 28.45 J/g) and azobenzene (Tm = 69.84°C) [26,27] and baselines were recorded using empty pans. Unless otherwise stated, the melting temperatures correspond to the maximum of the peak. Polymers were crushed and kept as powders under a dry atmosphere and for the measurements 4.9–5.1 mg of powder were placed in aluminum pans. For most measurements, the sample was kept melted during 15 min to erase its thermal history and subsequently cooled at 200°C/min to the selected crystallization temperature (T_c) where it was maintained for a predetermined time. Dry nitrogen cooled by passage through methanol at −40°C or liquid nitrogen was used for cooling. The melting curve was obtained by increasing the temperature at a rate of 20°C/min.

2.4. SAXS and WAXS

X-ray measurements were performed on the X33 double focusing monochromator-mirror camera [28] of the EMBL outstation on the storage ring DORIS of the Deutsches Elektronen Synchrotron (DESY) in Hamburg. WAXS and SAXS data were recorded simultaneously using two linear delay line readout detectors connected in series [29] covering the ranges of scattering vector ($s = 2 \sin \theta/\lambda$, where 2θ is the scattering angle and λ (0.15 nm) wavelength of the radiation) between 0.015 and 0.3 nm^{-1} in SAXS and 1.2 and 4 nm^{-1} in WAXS. The *s*-values corresponding to the detector channels were calibrated using jmtripalmitatin for WAXS and collagen for SAXS. The WAXS and SAXS spectra were normalized to the intensity of the primary beam using an ionisation chamber. Polymer samples (1 mm thick and 5 mm in diameter) were melted in aluminum pans and placed in a Mettler FP82 hot stage, which reproduced the temperature programs of the DSC experiments. Experimental data were analyzed using the OTOKO [30] and SAPOKO [31] programs.

2.5. NMR in solution

The spectra of the polymers in 1% deuterated

chloroform solutions were obtained with a Bruker WM250 spectrometer.

2.6. Density measurements

Density measurements were performed in aqueous outgassed $Ca(NO_3)_2 4H_2O$ solutions at room temperature using a Mettler Toledo DA-300M apparatus.

3. Results and discussion

3.1. Molecular weight

The number and weight average molecular weight and polydispersity of PCL, PHT and the copolymer are summarized in Table 1. The molecular weights were expressed in polystyrene units allow to estimate the number of PCL and PHT blocks in the copolymer. In first approximation, the copolymer is composed of two PHT and three PCL blocks separated by TDI units and is terminated by two of the three PCL blocks.

3.2. ^1H NMR in solution

The results are summarized in Table 2. The successive columns give the chemical shift of the different protons for PCL and PHT, their identification according to formulae I and II and the corresponding number of protons obtained by integration and the multiplicity of the bands (columns 1–4). The next columns (5–8) give the same parameters for the copolymer according to the proton numbering given in formula III.

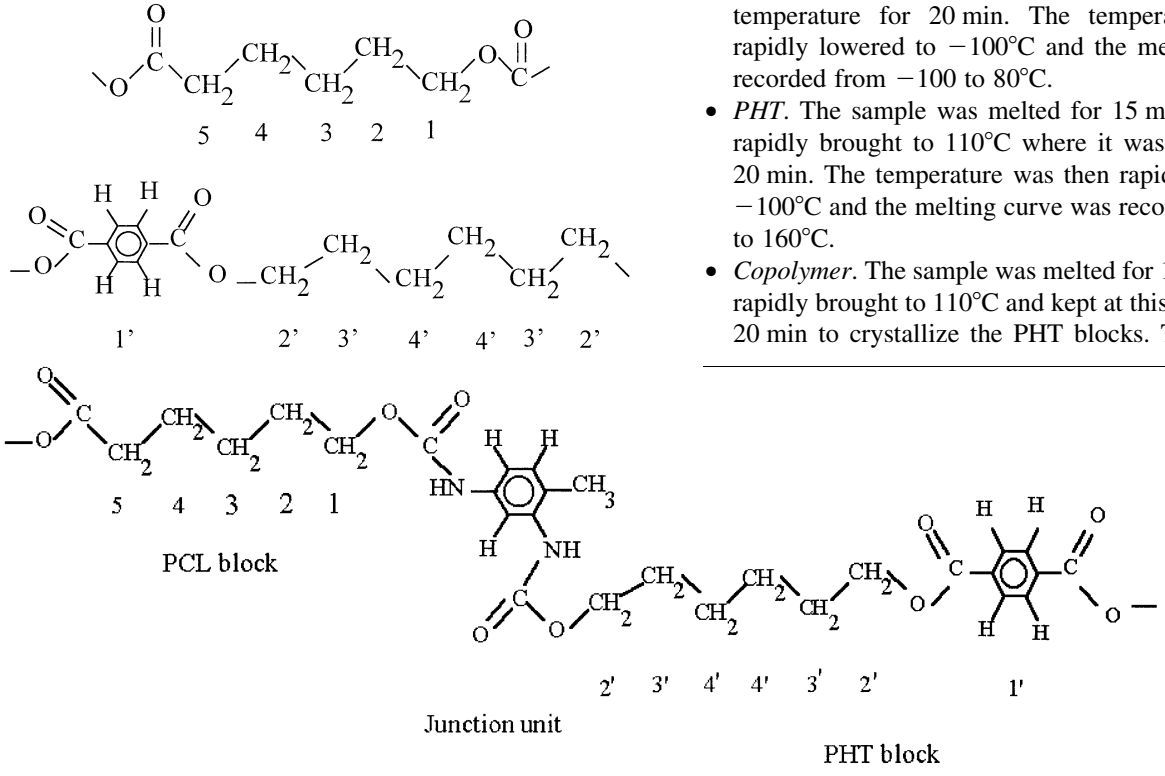

Table 1
Number and weight average molecular weight and polydispersity of PCL, PHT and the copolymer

Polymer	M_n [a]	$\bar{M}_n$ [b]	$\bar{M}_w$ [b]	Polydispersity
PCL	3000	6252	8335	1.33
PHT	3400	7537	13326	1.77
Copolymer	–	32,775	81,940	2.50

[a] Obtained by end-group titration.
[b] Expressed in polystyrene units.

Each of the peaks at 8.04, 4.25 and 1.80 ppm in the copolymer is associated with four protons of the PHT units. Integration of the peak of proton 5 at 2.22 ppm corresponding to the PCL units indicates that it is also associated to four protons. This means that the ratio of PCL to PHT monomers units in the copolymer is 2:1. Since the molecular weights of these monomer units are, respectively, 114 and 248, it can be deduced that the weight composition of the copolymer is 48/52 (PCL/PHT). Analysis of the complete signal between 1 and 2 ppm is in reasonable agreement with this hypothesis.

3.3. DSC

The diagrams obtained at heating rates of 20°C/min for PCL (A) and PHT (B) and at 20, 10 and 5°C/min (C–E) for the copolymer are given in Fig. 1. The thermal history of the samples is the following:

- *PCL*. The sample was melted for 15 min at 80°C, rapidly (−200°C/min) brought to 10°C and crystallized at this temperature for 20 min. The temperature was then rapidly lowered to −100°C and the melting curve was recorded from −100 to 80°C.
- *PHT*. The sample was melted for 15 min at 160°C and rapidly brought to 110°C where it was crystallized for 20 min. The temperature was then rapidly decreased to −100°C and the melting curve was recorded from −100 to 160°C.
- *Copolymer*. The sample was melted for 15 min at 180°C, rapidly brought to 110°C and kept at this temperature for 20 min to crystallize the PHT blocks. The temperature

Table 2
Parameters from ^{1}H NMR in solution

PCL and PHT				Copolymer			
Chemical shift (ppm)	Proton identification	Number of protons[a]	Multiplicity	Chemical shift (ppm)	Proton identification	Number of protons[a]	Multiplicity
8.08	1′	4	nR[b]	8.04	1′	4	nR
4.34	2′	4	nR	4.25	2′	4	3
4.06	1	2	3	3.98	1	4	3
2.31	5	2	3	2.22	5	4	3
1.81[c]	3′	4	nR	1.80[c]	3′	4	nR
1.65[d]	2 + 4	4	5 + 5	1.60	4′ + 2 + 4	4 + 4 + 4	nR
1.52	4′	4	nR				
1.38[c]	3	2	5	1.30[c]	3	4	5

[a] By integration.
[b] Non-resolved.
[c] Massif centered at the indicated chemical shift.
[d] Two quintets coinciding at 1.65 ppm.

was then rapidly lowered to 10°C, kept at this temperature for 20 min to crystallize the PCL blocks and then to −100°C. The melting curve was recorded from −100 to 180°C.

The curves obtained at 20°C/min (Fig. 1A–C) were examined for discontinuities and integrated to obtain T_g, T_{max}, the melting enthalpy ΔH_m and the crystallinity index expressed in percent of the total sample (Table 3). The values used for 100% crystalline PHT and PCL are, respectively, 143.1 [32] and 135.6 J/g [33].

Analysis of the curves obtained at 20°C/min (Fig. 1A–C) and of Table 3 reveals that:

- The glass transition temperature of PCL is higher in the copolymer than in pure PCL, possibly as a result of partial miscibility. T_g could not be measured for PHT in the copolymer since it is superimposed on the melting endotherm of the PCL blocks.
- Both PCL and PHT crystallize in the block material.
- The melting temperature of the blocks is lower than that of pure PHT and PCL. This could be due to a lower crystalline order, to different crystal populations or to partial miscibility.
- The crystallinity of the PCL blocks is much lower than that of pure PCL because the PCL blocks crystallize under stress in the PHT semi-crystalline network formed at higher temperature.

The shape of the endotherms obtained at 20°C/min (Fig. 1A–C) indicates that there is a multiple endotherm for pure PHT as well as for the PCL and PHT blocks in the copolymer. The effect of the heating rate on the shape of a multiple melting endotherm allows to identify the cause of the multiplicity. This multiplicity can be due either to polymorphism in the initial sample or to reorganization of one crystalline structure into another during heating [25,34]. Changes of the crystalline structure at the lattice level cannot be differentiated from modifications of the lamellar parameters by DSC and other methods like SAXS must be used. In the case of polymorphism, a lower heating rate increases the peak resolution and the maximum of the peak (T_{max}) occurs at a lower temperature. When reorganization occurs, a lower heating rate increases the yield of transformation of the least stable form into a more stable one, which melts at higher temperature, so that the relative proportion of the peaks changes with the heating rate.

In the case of pure PCL, there is one asymmetric peak with T_{max} at 54.0°C (Fig. 1A). When the heating rate decreases (not shown), the resolution increases and the tail of the peak separates as a shoulder, indicating polymorphism in the initial sample. The melting curve of PHT is more complicated (Fig. 1B) and a multiple endotherm consisting of successive exo- and endotherms with T_{max} at 142.1°C is observed. The proportion of the various components changes with the heating rate (not shown) and T_{max} decreases suggesting, respectively, complex reorganization and polymorphism. The thermal behavior of PHT and its copolymers with isophthalic acid (PHT-*co*-I) has been thoroughly investigated recently [25,34]. The results obtained in this last case confirm that the behavior of PHT and PHT-*co*-I is very complicated, involving both polymorphism and reorganization. In the present block copolymer, the proportion of the second PCL melting peak increases when the heating rate decreases (Fig. 1C–E), also suggesting melting reorganization. The first peak corresponds to the fraction crystallizing during cooling from 10 to −100°C whereas the second one, which is the most important one, corresponds to the fraction, which crystallizes at 10°C. In the PHT double melting endotherm region, a third peak appears when going from 20 to 10 or 5°C/min (Fig. 1C–E). The main characteristic of the PHT blocks melting is thus melting reorganization.

3.4. WAXS diagrams

Melting and crystallization have been thoroughly

Table 3
Thermal parameters obtained from Fig. 1A–C for PCL, PHT and the copolymer

Polymers	T_g (°C)	T_{max} (°C)		ΔH_m (J/g)		X (%)	
PHT	–	142.1		56.8		40	
PCL	−48.2	54.0		100.9		74	
Copolymer	−39.0	PHT blocks 135.8	PCL blocks 40.6	PHT blocks 40.0	PCL blocks 38.3	PHT blocks 28	PCL blocks 28

investigated as a function of time using WAXS, four diagrams being recorded per minute during crystallization and one during melting. The thermal history of the sample was the same as that used for the DSC experiments except that a cooling rate of 20°C/min instead of 200°C/min was used for all samples. The lower temperature was 0°C for PCL, 60°C for PHT and −20°C for the copolymer instead of −100°C. The heating rate used to record to WAXS diagrams was 1°C/min in all cases. These conditions,

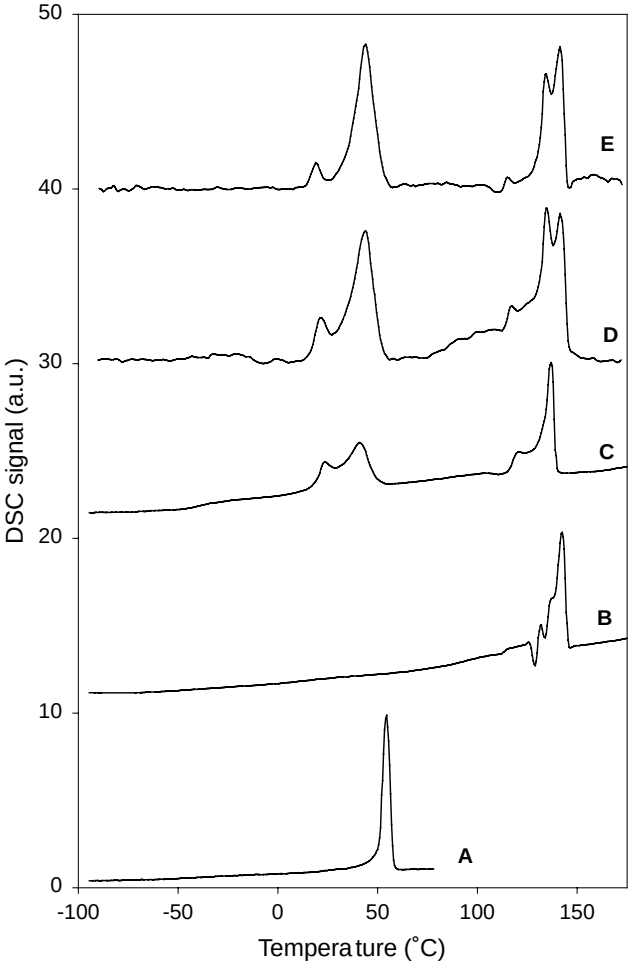

Fig. 1. DSC diagrams obtained at an heating rate of 20°C/min for PCL (A) and PHT (B) and at 20, 10 and 5°C/min (C)–(E) for the PCL–PHT copolymer. The curves have been displaced along ordinate for better visualization.

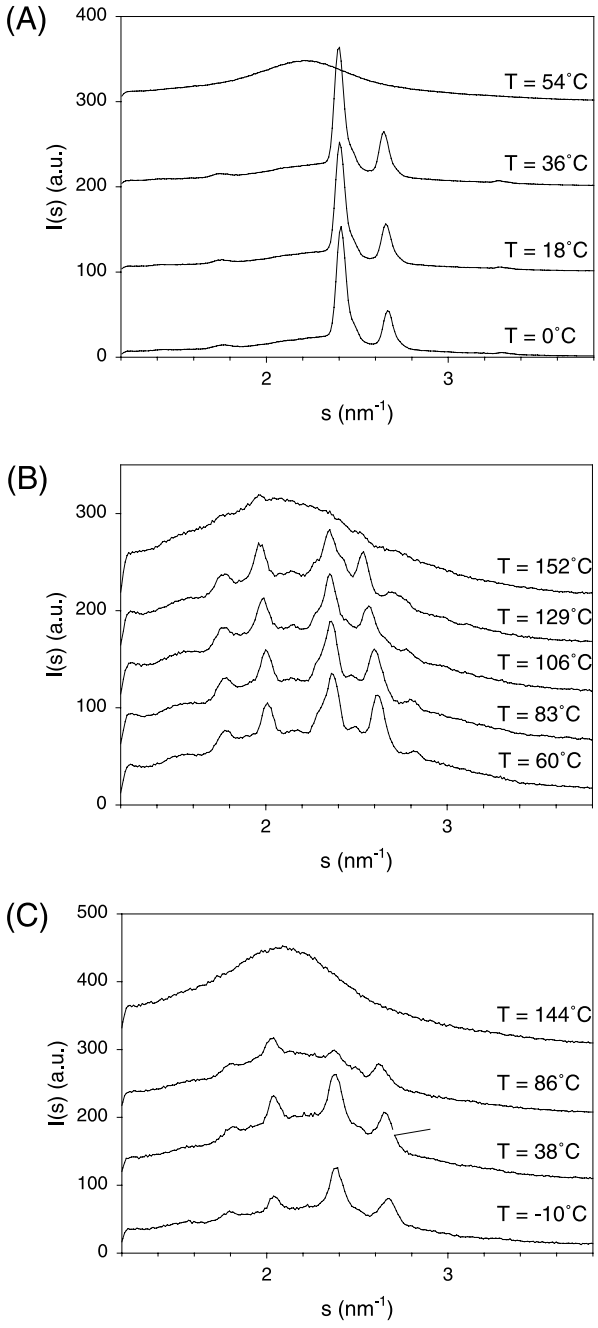

Fig. 2. WAXS profiles taken during the melting of PCL (A), PHT (B) and the PCL–PHT copolymer (C). The curves have been displaced along ordinate for better visualization.

Table 4
Assignment of the PHT peaks according to Ref. [32]

Peaks	$d(PHT)_{exp}$ (nm)	$d(PHT)_{ref}$ (nm)	(*hkl*)	System
1	0.547±0.002	0.570	111	Monoclinic
2	0.487±0.002	0.502	100	Triclinic
3	0.415±0.002	0.412	130	Monoclinic
Shoulder	0.432±0.002	0.425	101	Triclinic
		0.427	201	Monoclinic
4	0.376±0.004	0.385	110	Triclinic
		0.380	220	Monoclinic

Table 5
Assignment of the PCL peaks according to Ref. [35]

Peaks	$d(PCL)_{exp}$ (nm)	$d(PCL)_{ref}$ (nm)	(*hkl*)
1	0.415 ± 0.002	0.412	110
2	0.374 ± 0.002	0.371	200

which are different from those used in the DSC measurements, were chosen for practical reasons. In the present conditions, PCL blocks display a single endotherm with T_{max} at 42.8°C and PHT a triple one with T_{max} at 133°C (not shown). The crystallinities of the PCL and PHT blocks are, respectively, 30 and 17%. The melting endotherms for pure PCL and PHT (not shown) are in agreement with those found in the preceding conditions.

Typical WAXS diagrams are given in Fig. 2A–C. Owing to the long crystallization time and the low heating rate, the diagrams corresponding to crystallization at a given temperature are similar to those for melting. Therefore, only melting WAXS diagrams are detailed here. Melting of PHT, PCL and the block components are clearly identified by the progressive disappearance of the crystalline peaks and their replacement by a broad halo. These diagrams were used to calculate the lattice parameters and their variation with temperature. Combining crystallinity measurements, values of the lattice parameters and density measurements, the measured density could be compared with the calculated one.

3.5. Lattice parameters

The *d*-spacings given in Tables 4–6 for PCL at 25°C and for PHT at 60°C and for the copolymer at different temperatures were calculated from the WAXS diagrams. The corresponding diffraction planes and crystalline systems have been identified using data from the literature [32,35]. For PCL, only one crystalline system is involved (orthorhombic). The two resolved peaks for PCL (110 and 200) correspond exactly to two of the four peaks of PHT (130 monoclinic at 0.415 nm, 110 triclinic and 220 monoclinic at 0.376 nm). Comparison of the data of Tables 4–6 indicates that the two blocks melt and crystallize independently in the copolymer. Indeed, the *d*-spacings in the copolymer are identical to those of the building PHT and PCL blocks. The experimental *d*-values were calculated for different temperatures using the standard formulae [36]. The *c*-parameter for the triclinic PHT and for PCL could not be obtained since the required reflections were missing. Values of *c* reported in the literature for PCL [35] and for PHT [32] were used to calculate the *a*- and *b*-values from our WAXS data. The resulting lattice parameters are given in Table 7 and compared with data from the literature. The values of *a* and *b* were then calculated in the entire experimental temperature range. The variation was only significant for the monoclinic *a*-value and the triclinic *b*-value corresponding to PHT and the copolymer. It amounts to ±5% between 60 and 160°C for PHT and ±8% between −10 and 160°C for the copolymer and is negligible in the other cases.

3.6. Density measurements

Using the crystallinity index measured by DSC, the density of the crystalline phases (d_c) calculated from the lattice parameters obtained from WAXS and the density of the amorphous phase (d_a) calculated from group contributions [37], the global density (d_{calc}) of PHT, PCL and the copolymer was computed and compared with the value (d_{exp}) obtained directly from the density measurements. For the copolymer, the previously determined weight fraction was also used and it was assumed that the contributions of the monoclinic and triclinic crystal phases to the PHT blocks are equivalent. The results are summarized in Table 8. Comparison of the last two columns indicates that the calculated values are in agreement with the experimental ones. These results provide an additional proof of the independent behavior of the two types of blocks in the copolymer.

3.7. SAXS

This method allows to identify changes in the lamellar structure as a function of temperature and to compare the lamellar structure of the copolymer with that of pure PCL and PHT. Typical SAXS diagrams as a function of temperature are given in Fig. 3A–D. The thermal history of the sample was identical to that used for WAXS since both types of diagrams were recorded simultaneously on the same sample.

For PCL and PHT (Fig. 3A and B), one broad peak due to superposition of lamellae is observed at the lower temperatures. The absence of second-order peaks in PHT suggests a poor regularity of the lamellar staking. The PHT peaks are broader than those of PCL indicating a broader distribution of the lamellar thickness for PHT. The mean periodicity of the lamellar system calculated using Bragg's law is given in Table 9 at −10°C for the PCL and 60°C for the PHT. These spacings were also found, together with the thickness of the crystalline and amorphous layer (l_c and l_a), by analysis of the linear correlation function [38]. The linear degree of crystallinity ϕ_L in the lamellar stacks is given by $l_c/(l_c + l_a)$, where l_c and l_a are the thickness of the crystalline and amorphous

Table 6
Assignment of the PCL and PHT peaks in the block copolymer according to Ref. [32] and Ref. [35]

d_{exp} (nm)				d_{ref}, PHT (Palmer), PCL (Bittiger) (nm)		
Peak	−10°C	80°C	110°C	−10°C	80°C	110°C
1	0.556	0.556	0.558	0.570 PHT (monoclinic (111))		
2	0.490	0.493	0.502	0.502 PHT (triclinic (100))		
3	0.420	0.420	0.418	0.412 PCL (110), 0.412 PHT (monoclinic (130))	0.412 PHT (monoclinic (130))	0.412 PHT (monoclinic (130))
4	0.374	0.380	0.390	0.371 PCL (200)	0.380 PHT (monoclinic (220)), 0.385 PHT (triclinic (110))	0.385 PHT (triclinic (110))

Table 7
Comparison of the crystalline parameters calculated from the WAXS diagrams and obtained from the literature [32,35]

Polymer	Calculated parameters (Å)									Literature parameters (Å)					
	a			*b*			*c*			*a*		*b*		*c*	
PHT	T	M		T	M		T	M		T	M	T	M	T	M
	5.1	8.9		5.9	17.8		–	14.2		5.2	9.1	5.3	17.6	15.7	15.7
PCL	7.5			5.0			–			7.5		5.0		17.3	
Copolymer	T	M	O	T	M	O	T	M	O	–		–		–	
	5.1	8.8	7.5	5.9	18.2	5.1	–	14.9	–						

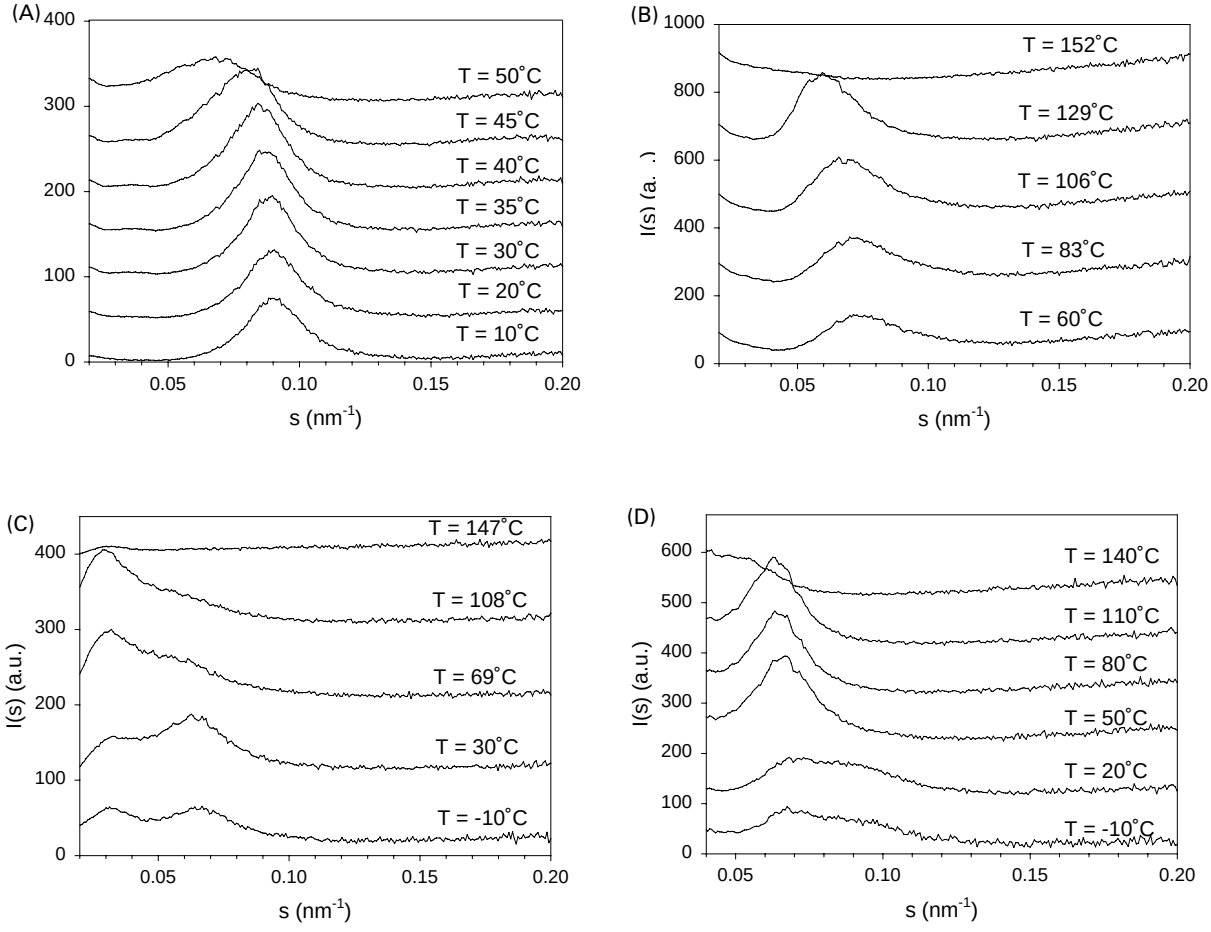

Fig. 3. SAXS profiles taken during the melting of PCL (A), PHT (B), the PCL–PHT copolymer (C) and the mechanical blend of PCL and PHT (D). The curves have been displaced along ordinate for better visualization.

Table 8
Comparison of the experimental and calculated densities

	d_a	d_c	d_{exp}	d_{calc}
PCL	1.09	1.17	1.15	1.15
PHT	1.18	1.40 (monoclinic), 1.26 (triclinic)	1.24	1.24 (monoclinic), 1.20 (triclinic)
PCL blocks	1.09	1.15		1.15
PHT blocks	1.18	1.32 (monoclinic), 1.20 (triclinic)		1.21 (monoclinic), 1.18 (triclinic)
Copolymer			1.15	1.16

regions in the stacks. It can be compared with the mass (X) and volume macroscopic (ϕ) crystallinities obtained from DSC measurements (related by $X = \phi d_c/d$). The values of ϕ_L and ϕ indicate that the PHT sample is filled with lamellar stacks of low crystalline content, whereas the PCL sample contains highly crystalline lamellar stacks.

At a temperature of 30°C corresponding to the beginning of the DSC melting curve, the SAXS maximum of PCL becomes slightly broader and shifts to larger long periods indicating melting reorganization as proposed in Section 2 from the comparison of the DSC melting curves obtained at different heating rates. Some of the diagrams obtained for the melting of the copolymer are given in Fig. 3C. At low temperature, two peaks are observed but the second one is not the second order of the first one and their relative intensities vary strongly as a function of temperature. This suggests the existence of two crystal populations with different lamellar thickness distributions in the copolymer. This interpretation is supported by the comparison of the temperature evolution of the copolymer (Fig. 3C) and of a mechanical blend of PCL and PHT (Fig. 3D). The position of the peaks is different in both cases. In the latter, the first and second peaks can, respectively, be assigned to PHT and PCL since the corresponding long periods are those observed for the individual polymers. Crystallization of the blend is thus accompanied by complete phase separation of the two components in two domains containing, respectively, PCL and PHT domains. In the SAXS pattern of the copolymer, the smaller long period corresponds closely to the distance between PCL and PHT blocks, whereas the longer period corresponds to the overall periodicity, including the two crystalline regions separated by amorphous zones. These findings are also supported by the simulations of correlation functions based on the electron density profiles presenting two alternating different crystal zones [39].

Table 9
Crystallinity parameters of PCL and PHT in the synchrotron conditions

	PCL (after crystallization at 10°C)	PHT (after crystallization at 110°C)
Bragg long period (nm)	11	14
Correlation functions analysis		
l (nm)	10.5	12.2
l_c (nm)	6.3	3.3
l_a (nm)	4.2	8.9
Linear stack crystallinity, ϕ_L (%)	60	27
DSC weight crystallinity, X (%)	70	31
DSC volume crystallinity, ϕ (%)	69	30

4. Conclusions

Under the crystallization conditions used in the present work, PCL, PHT and the copolymer display a complex behavior. The glass transition temperature is higher for the PCL blocks than for the copolymer suggesting partial miscibility of the blocks. Both PCL and PHT crystallize in the block material but a decrease of the melting temperature is observed indicating a lower crystalline order, a different crystal population or partial miscibility. The crystallinity of PCL blocks is much lower than that of pure PCL because they crystallize under stress in the PHT semi-crystalline network.

WAXS diagrams indicate that PCL and PHT crystallize independently in the copolymer, the lattice parameters being identical in the blocks and in pure PHT and PCL. Using these lattice parameters, the density of the crystalline phases could be calculated. Combining these values with the density of the amorphous phases calculated from group contributions and the crystallinity index measured by DSC, values of the densities of PHT, PCL and the copolymer were obtained and compared with the measured ones. A good agreement is obtained, which also indicates that the blocks behave independently in the copolymer. The presence of two independent SAXS peaks before the melting of PCL blocks suggests that in the copolymer, two alternate crystal populations with a different lamellar thickness distributions coexist. The smaller long period corresponds to the mean periodicity between two crystalline blocks of different chemical composition. The longer one corresponds to the periodicity between crystalline blocks of the same nature. This interpretation is supported by comparison of the SAXS diagrams as a function of temperature of the block copolymer and of a mechanical blend of pure PCL and PHT. The calculated correlation functions for such a model is also in agreement with experimental ones obtained for the copolymer [39].

Acknowledgements

We thank the 'Fonds pour la Formation à la Recherche dans l'Industrie et dans l'Agriculture' (FRIA) for a grant to C. Lefèvre. This work was done with the support of the European Union through the HCMP Access to Large Installations Project, contract CHGE-CT93-0400 to the Hamburg Outstation of European Molecular Biology Laboratory. C.L. and C.D. are very grateful to Prof. H. Reynaers

(KU Leuven) for the opportunity to use his equipment for the synchrotron experiments and his support.

References

[1] Seal KJ. Biodegrad Abstr 1988:2–25.
[2] Potts JE. In: Jellinek HHG, editor. Aspects of degradation and stabilization of polymers. Amsterdam: Elsevier, 1978.
[3] Chiellini E, Corti A, Giovannini A, Narducci P, Paparella AM, Solaro R. J Environ Polym Degrad 1996;4(1):37–54.
[4] Jun HS, Kim BO, Kim YC, Chang HN, Woo SI. J Environ Polym Degrad 1994;2(1):9–18.
[5] Chauret C, Mayfield I, Inness WE. Can J Microbiol 1995;41(1):54–63.
[6] Keyser P, Pujar BG, Eaton RW, Ribbons DW. Environ Health Perspect 1976;18:159–66.
[7] Ganji SH, Karigar CS, Pujar BG. Biodegradation 1995;6:61–6.
[8] Karegoular TB, Pujar BG. FEMS Microbiol Lett 1985;30:217–20.
[9] Schaläfli HR, Weiss MA, Leisinger T, Cook AM. J Bacteriol 1994;176(21):6644–52.
[10] Lefèvre C, Mathieu C, Tidjani A, Dupret I, Vander Wauven C, De Winter W, David C. Polym Degrad Stab 1999;64:9–16.
[11] Nikida H, Tokiwa Y. J Environ Polym Degrad 1993;1(3):227–33.
[12] David C, Dupret I, Lefèvre C. Macromol Symp 1999;144:141–51.
[13] Bastioli C, Cerutti A, Guanalla I, Romano GC, Tosin M. J Environ Polym Degrad 1995;3:81–95.
[14] Witt U, Müller RJ, Deckwer WD. J Environ Polym Degrad 1995;3(4):215–25.
[15] Fairclough JPA, Hamley IW, Terril NJ. Radiat Phys Chem 1999;56:159–73.
[16] Goodman I, editor. Developments in block copolymers. New York: Applied Science, 1970.
[17] Leibler I. Macromolecules 1980;13:1602–17.
[18] Rosendale JH, Bates FS, Almdal K, Mortensen K, Wignall D. Macromolecules 1995;28:1429–43.
[19] Nojima S, Kato K, Yamamoto S, Ashida T. Macromolecules 1992;25:2237–42.
[20] Rangarajan P, Register R, Felters LJ. Macromolecules 1993;26:4640–5.
[21] Rangarajan P, Register R, Adamson DH, Fetters LJ, Bras W, Naylor S, Ryan AJ. Macromolecules 1995;28:1422–8.
[22] Ryan AJ, Hamley IW, Bras W, Bates FS. Macromolecules 1995;28:3860–8.
[23] Ryan AJ, Fairclough JPA, Hamley IW, Mai S, Booth C. Macromolecules 1997;30:1723–7.
[24] Nojima S, Ono M, Ashida T. Polym J 1992;24:1272–80.
[25] Lefèbvre X, Koch MHJ, Reynaers H, David C. J Polym Sci, Part B: Polym Phys 1999;37:1–18.
[26] Mathot VBF. Calorimetry and thermal analysis of polymers. Munich: Hanser, 1994 (chapter 5).
[27] Höhne G, Hemminger W, Flammersheim H-J. Differential scanning calorimetry: an introduction for practioners. Berlin: Springer, 1996.
[28] Koch MHJ, Bordas J. Nucl Instrum Meth 1983;208:461–9.
[29] Rapp G, Gabriel A, Dosiere M, Koch MHJ. Nucl Instrum Meth Phys Res 1995;A357:178–82.
[30] Boulin C, Kempf R, Koch MHJ, Mc Laughlin SM. Nucl Instrum Meth 1986;A249:399–407.
[31] Koch MHJ, Svergun D. 1999 (unpublished).
[32] Palmer A, Dandurand SP, Revol JF, Brise F. Eur Polym J 1984;20(8):783–9.
[33] Benedict V, Cook WJ, Jarret P, Cameron JA, Huang SJ, Bell JP. J Appl Polym Sci 1983;28:327–34.
[34] David C, Lefèbvre X, Lefèvre C, Demarteau W, Lautz J-M. Prog Org Coatings 1999;35:45–54.
[35] Bittiger H, Marchessault RH, Niegisch WD. Acta Crystallogr 1970;B26:1923–7.
[36] Wunderlich B. Macromolecules physics, vols. 1–3. New York: Academic Press, 1973.
[37] Van Krevelen DW. Properties of polymers. 3rd ed. Amsterdam: Elsevier, 1990 (chapter 4).
[38] Strobl GR, Schneider MJ, Martin GV. J Polym Sci, Polym Phys Ed 1980;18:1361–81.
[39] Villers D, et al. (in preparation).